

非晶與奈米晶多層膜結構在壓縮測試下之 機械性質與變形行為

Mechanical Properties and Deformation Behaviors in Amorphous/Nanocrystalline Multilayer under Microcompression

Student: M. C. Liu

Adviser: Prof. Huang

04/23/2011

*Department of Materials and Optoelectronic Science
National Sun Yat-Sen University (NSYSU)*

Research motive

Amorphous/crystalline nanolaminates

- ◆ **Composite concept might be one of the ways to solve this dilemma.** Analyses of mechanical properties and deformation behaviors of the multilayer (**amorphous/crystalline**) micropillars are another purpose in this study.
- ◆ **BMG + Nano-metals = ???**

Nanolaminates

- ➔ **high potential for structural applications**
- ➔ **interesting model system**

Research motive

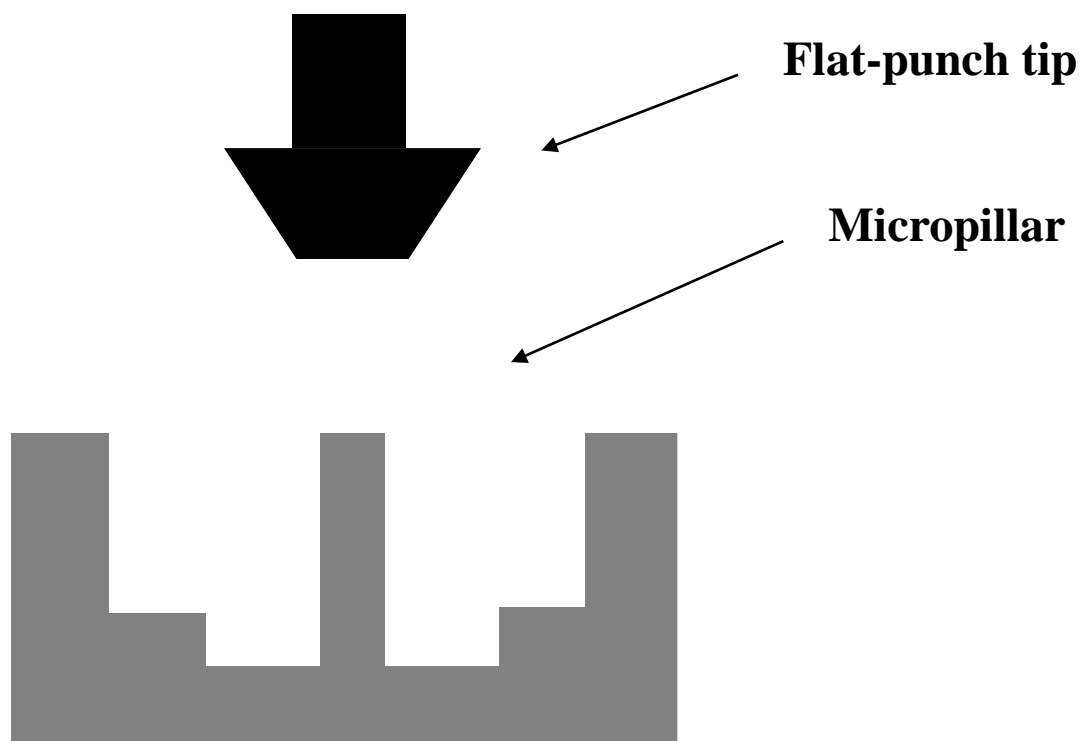
Amorphous/crystalline nanolaminates

- ◆ The **size-scale or thickness effects** on deformation behaviors for multilayer thin films should be further investigated. If the critical thickness of individual layer can be defined, it is expected that the larger plasticity on amorphous/crystalline micropillar can be observed.
- ◆ The critical sample size below which shear band localization would disappear and the sample can deform homogeneously on metallic glasses.

 in situ TEM compression tests (**Nanocompression**)

What is microcompression test?

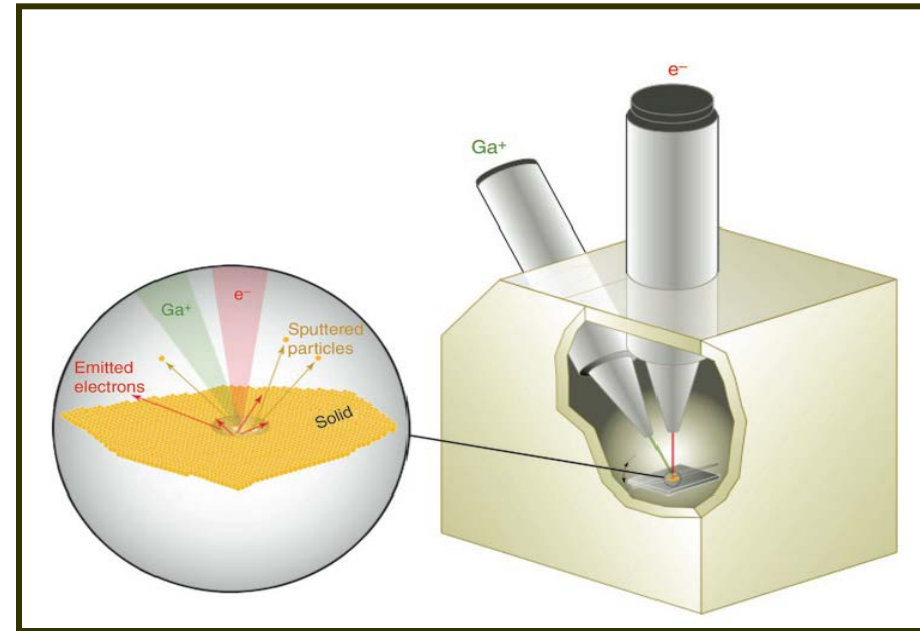
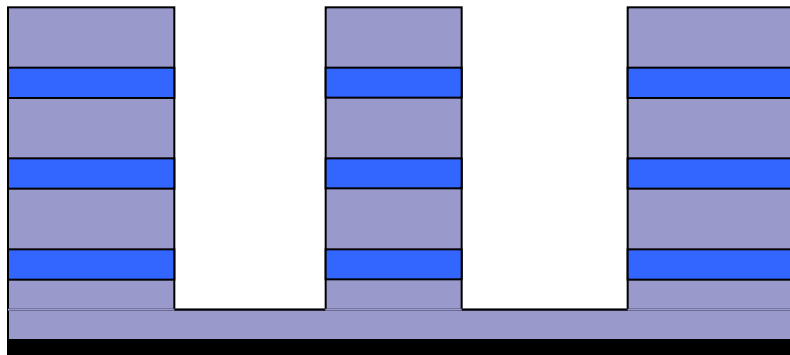
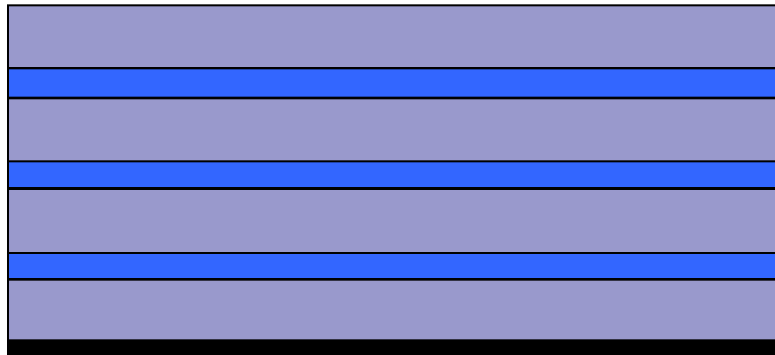
This technique, developed by **Uchic et al.** in 2004, was first applied to examine the mechanical properties of micrometer sized sample.



Experiments



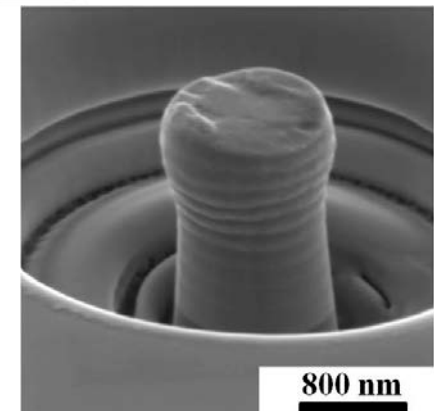
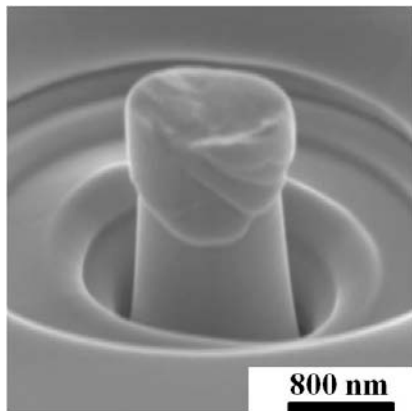
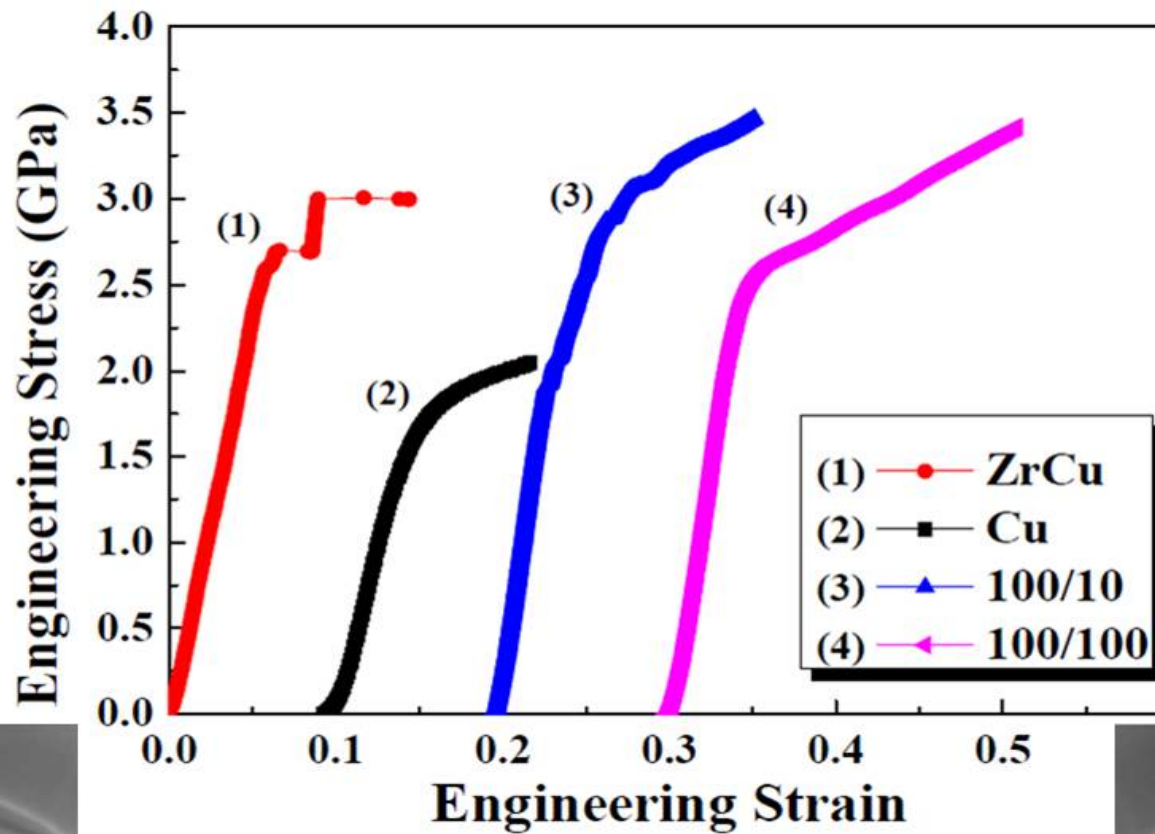
Focused ion beam micromachining



Results and discussion

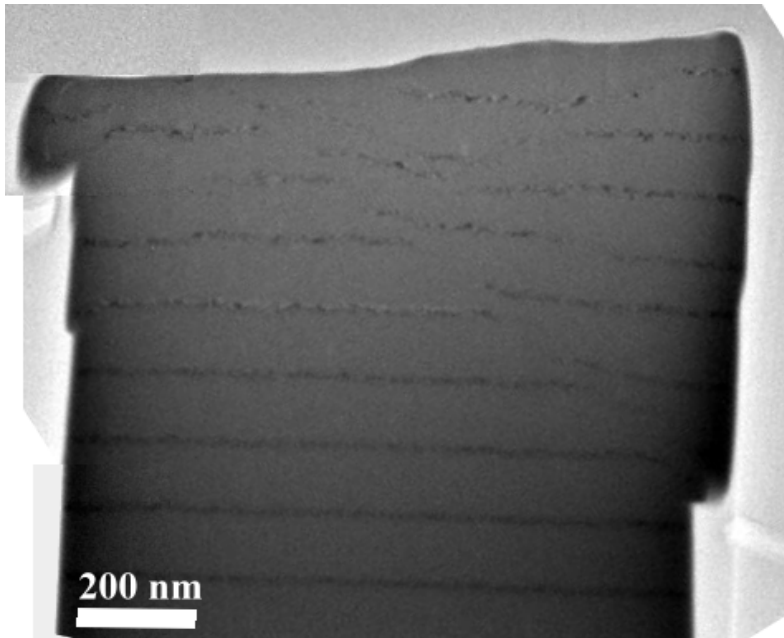
- ▶ **Microcompression tests on multilayer pillars**

Results for ZrCu/Cu micropillar

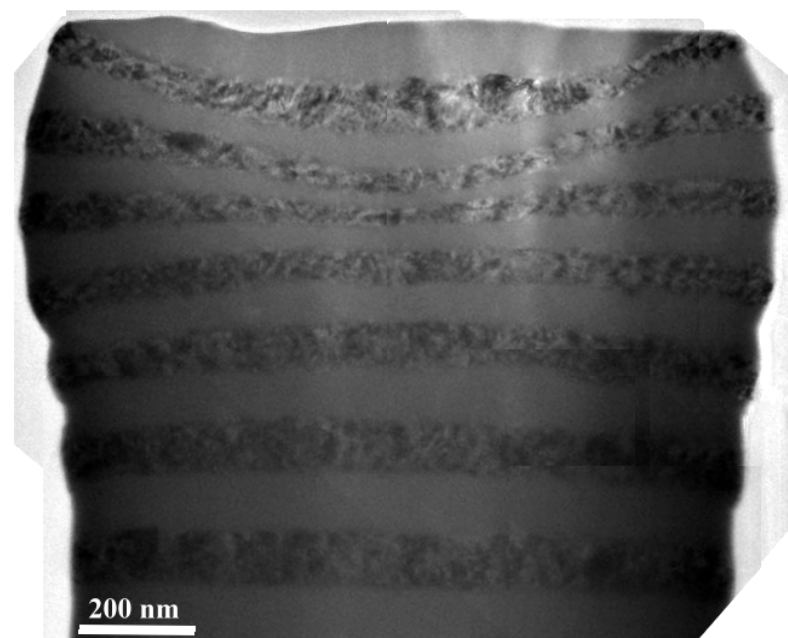


Results for ZrCu/Cu micropillars

100/10 nm

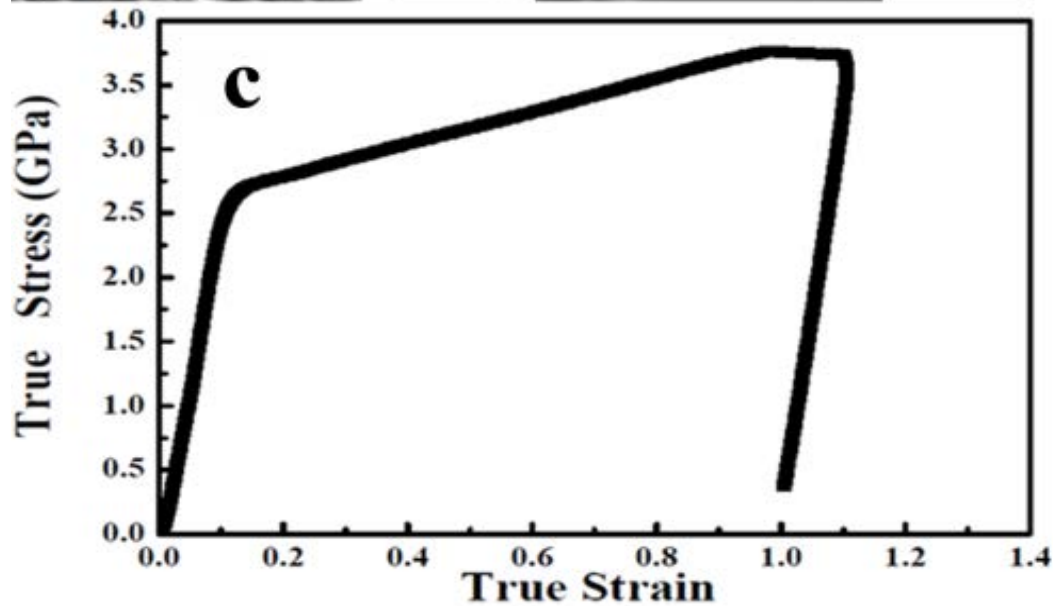
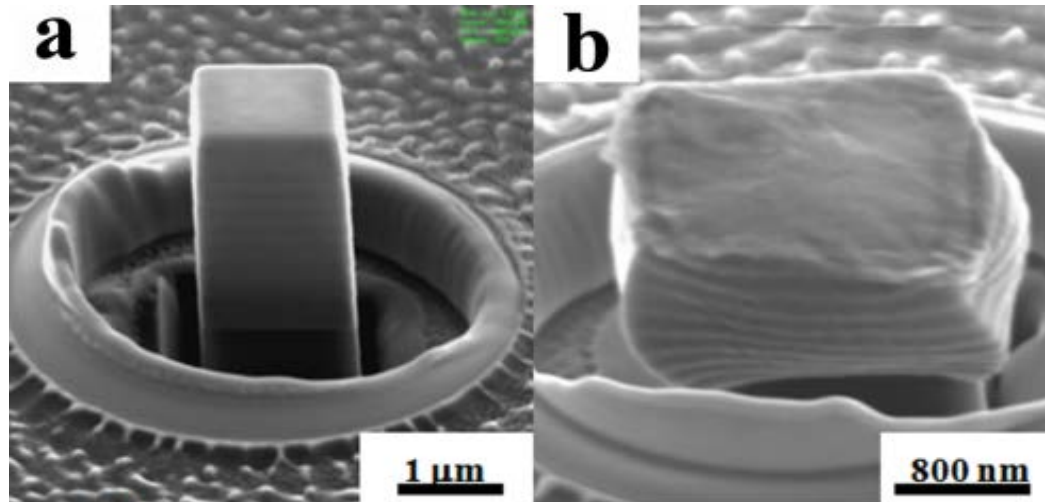


100/100 nm

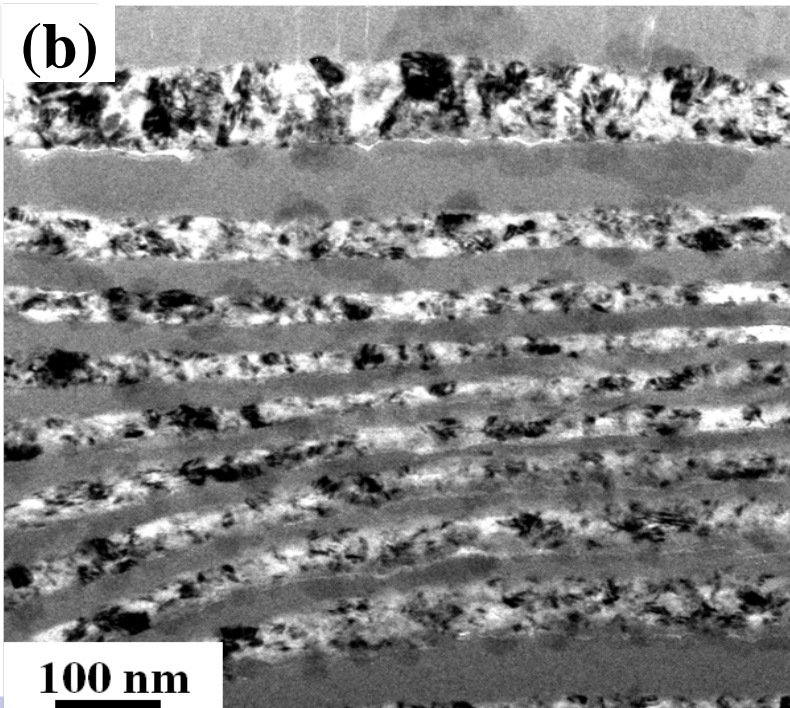
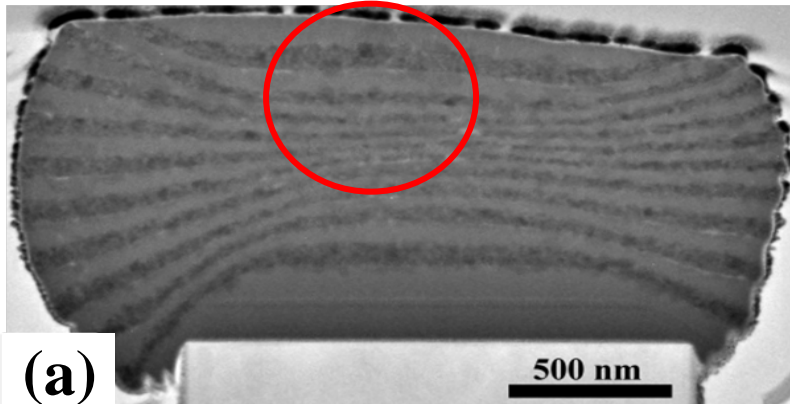


TEM micrographs showing the appearances of the deformed 100/10 nm and 100/100 nm ZrCu/Cu round micropillars.

ZrCu/Cu 100/100 nm rectangular micropillar

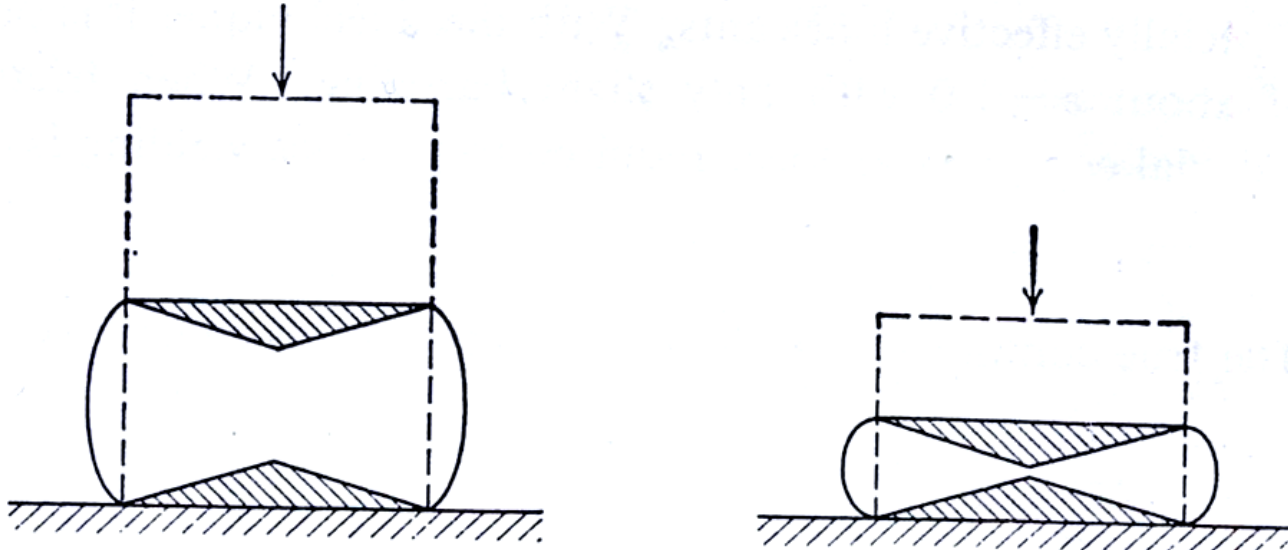


ZrCu/Cu 100/100 nm rectangular micropillar



(a) TEM micrographs showing the appearances of the deformed 100/100 nm ZrCu/Cu rectangular micropillars. (b) High-magnitude TEM image of the circular region marked in Figure (a).

Barreling effect on ductile materials



Undeformed regions (shaded) due to friction at ends of a compression specimen.

Results and discussion

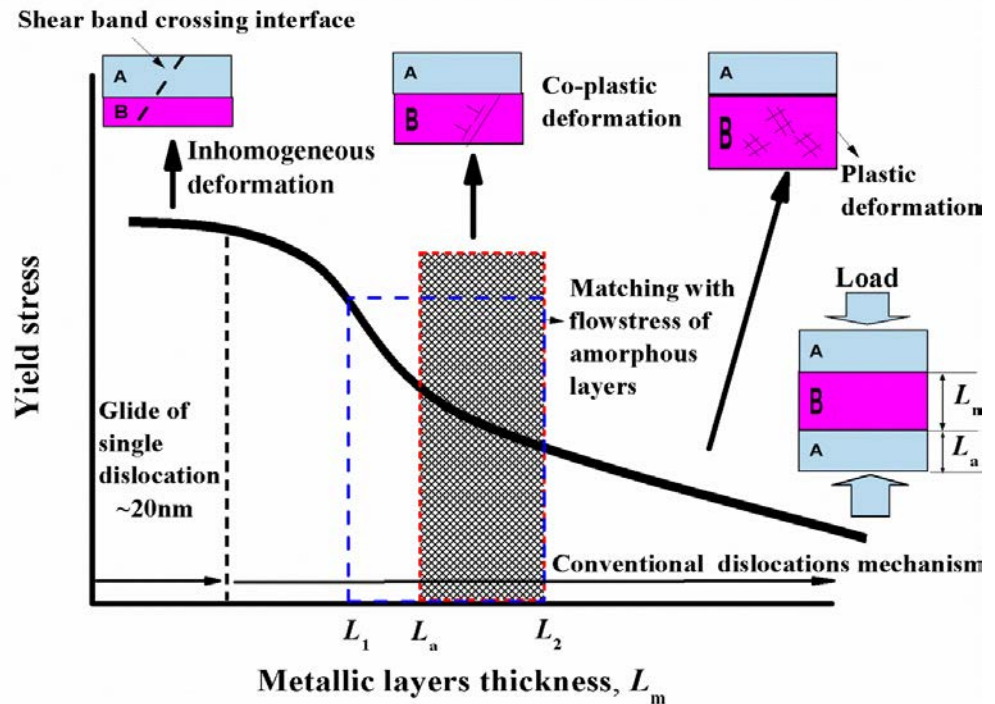
◆ Hall-Pitch relationship between flow stress σ and the thickness of layers L_m : $\sigma \propto L_m^{-1/2}$.

(Misra et al., Acta Mater., 2005)

(Misra et al., JOM, 2008)

◆ For the current case:

- $L_a \leq L_m$
- $L_1 \leq L_m \leq L_2$
- $L_a = 100 \text{ nm} = L_m$

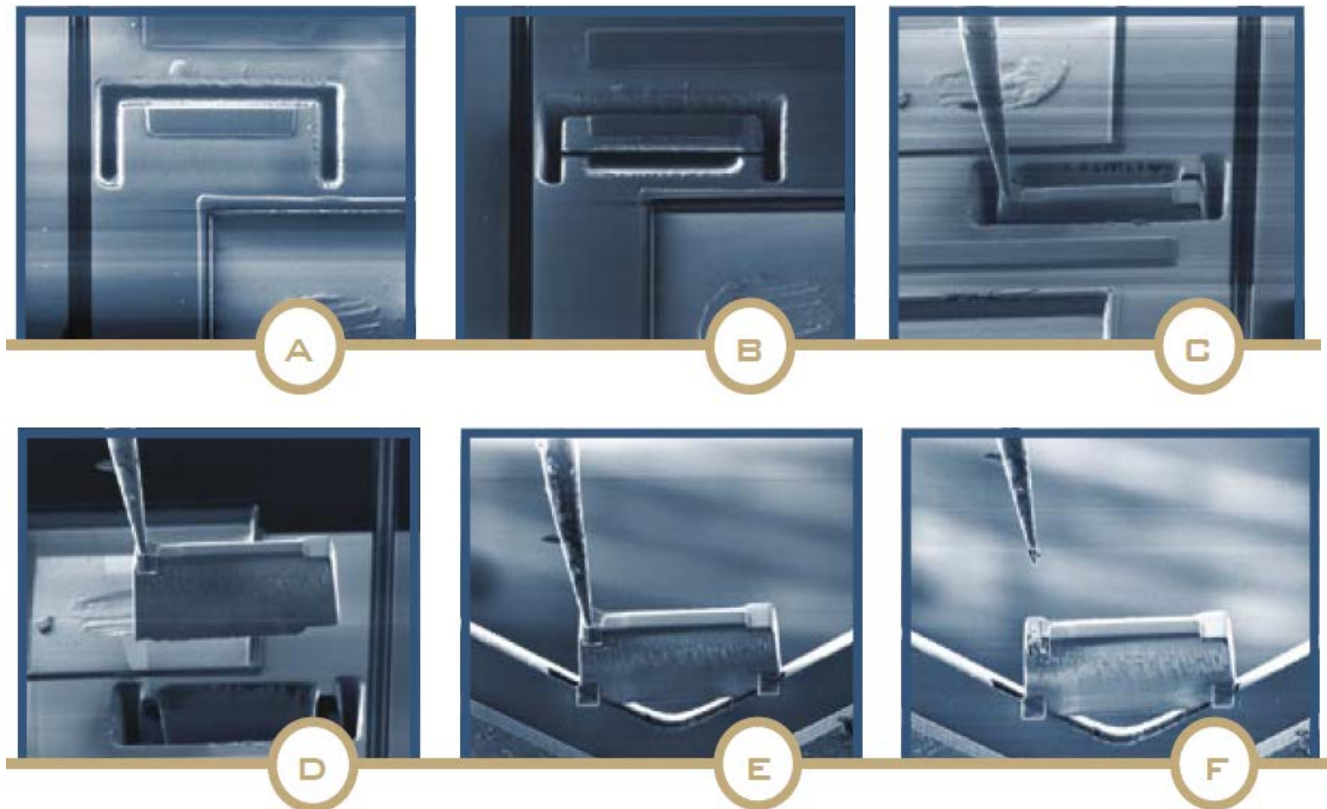


Schematic illustration of the deformation mechanism in the metallic amorphous/crystalline nanolayered composites as a function of metallic layers thickness.

Results and discussion

- ▶ **In situ TEM compression tests on ZrCu TFMGs**

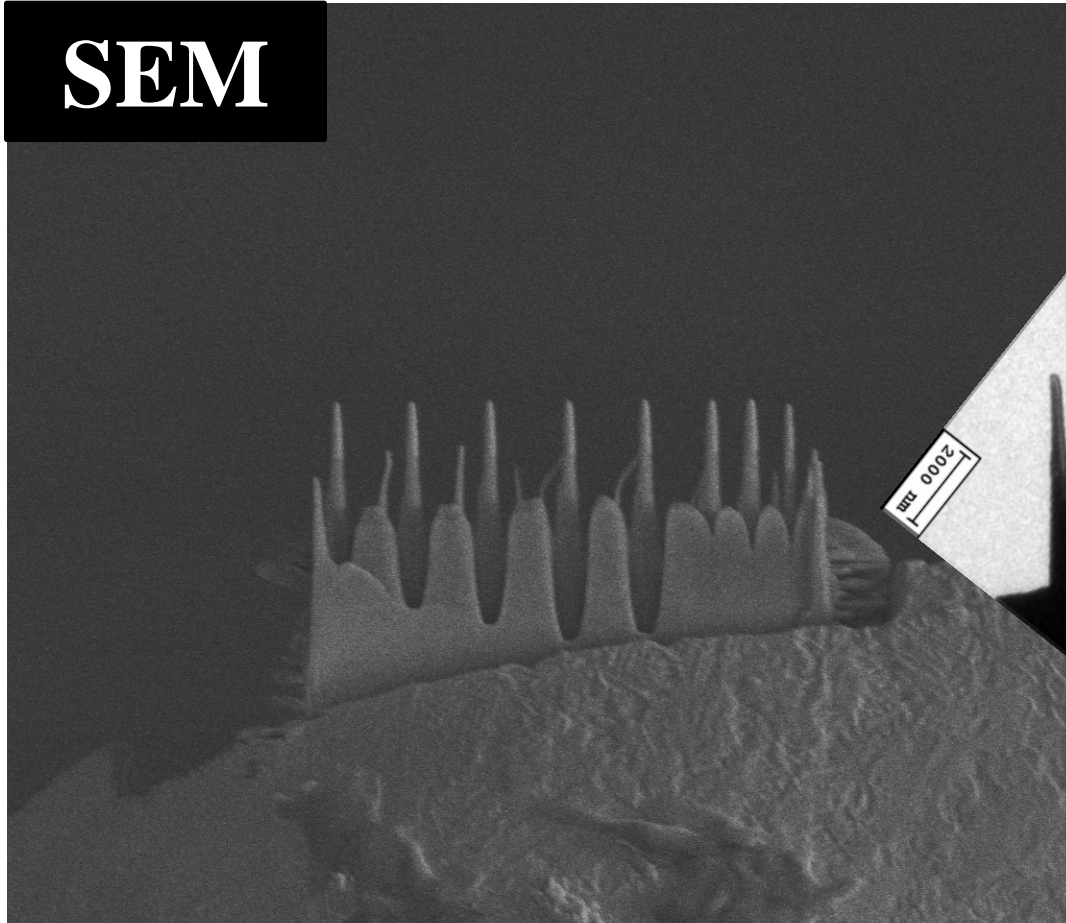
In-situ lift-out method



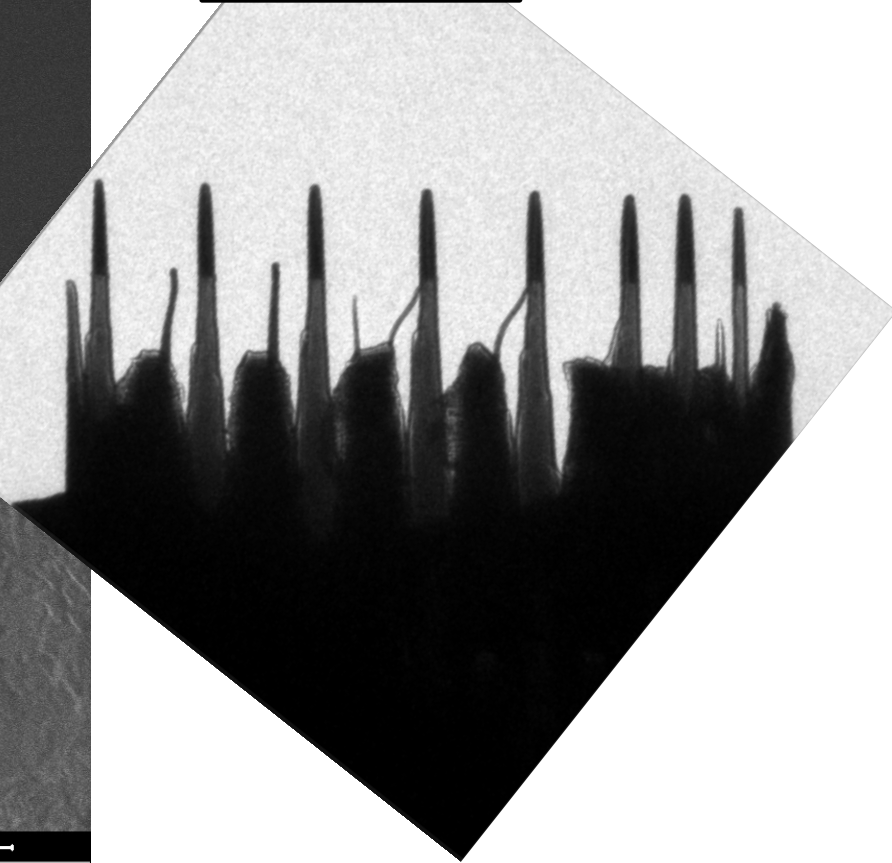
Typical six steps of in situ lift-out method: (A) first cut; (B) release cut; (C) tip attach; (D) extraction; (E) holder attach; (F) and tip separation.

In situ TEM samples

SEM



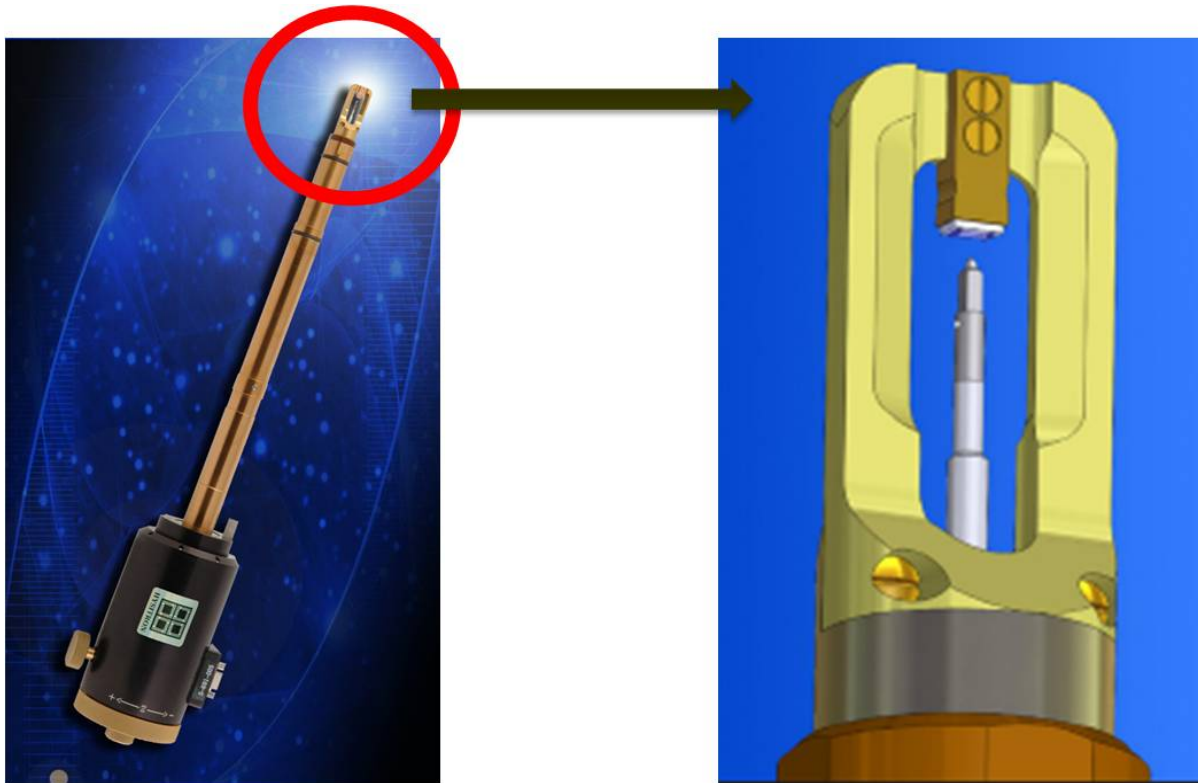
TEM



WD	mag	HV	tilt	HFW	8/4/2010
4.8 mm	5 000 x	5.00 kV	52 °	25.6 μm	4:56:58 PM

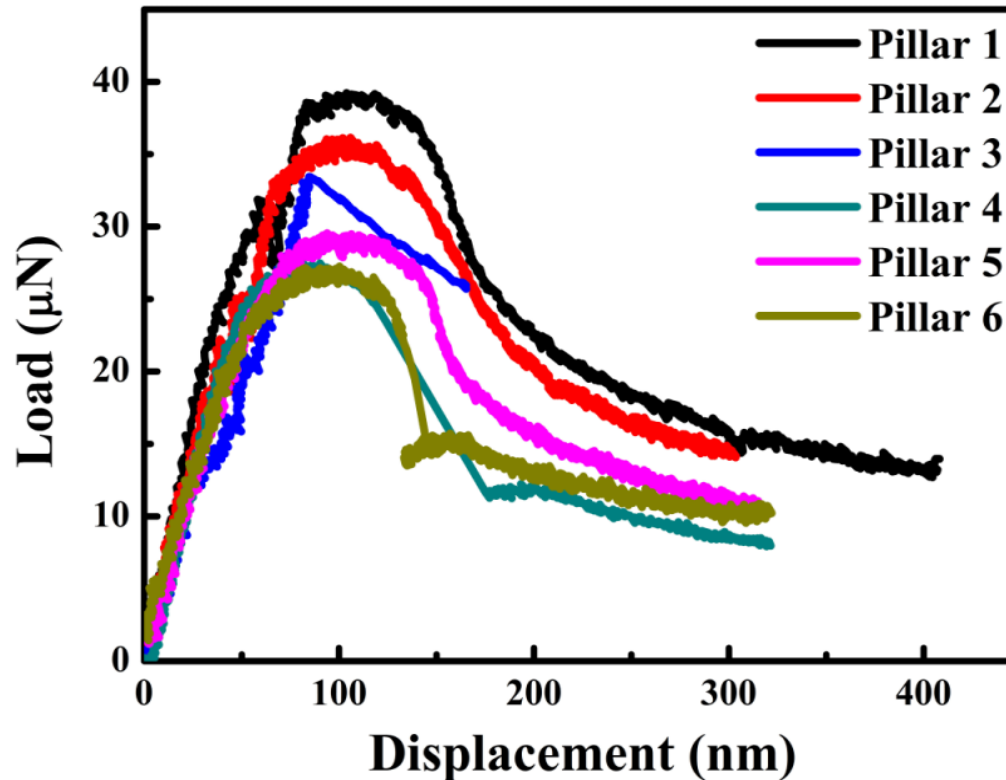
5 μm
SEM

Holder specifications



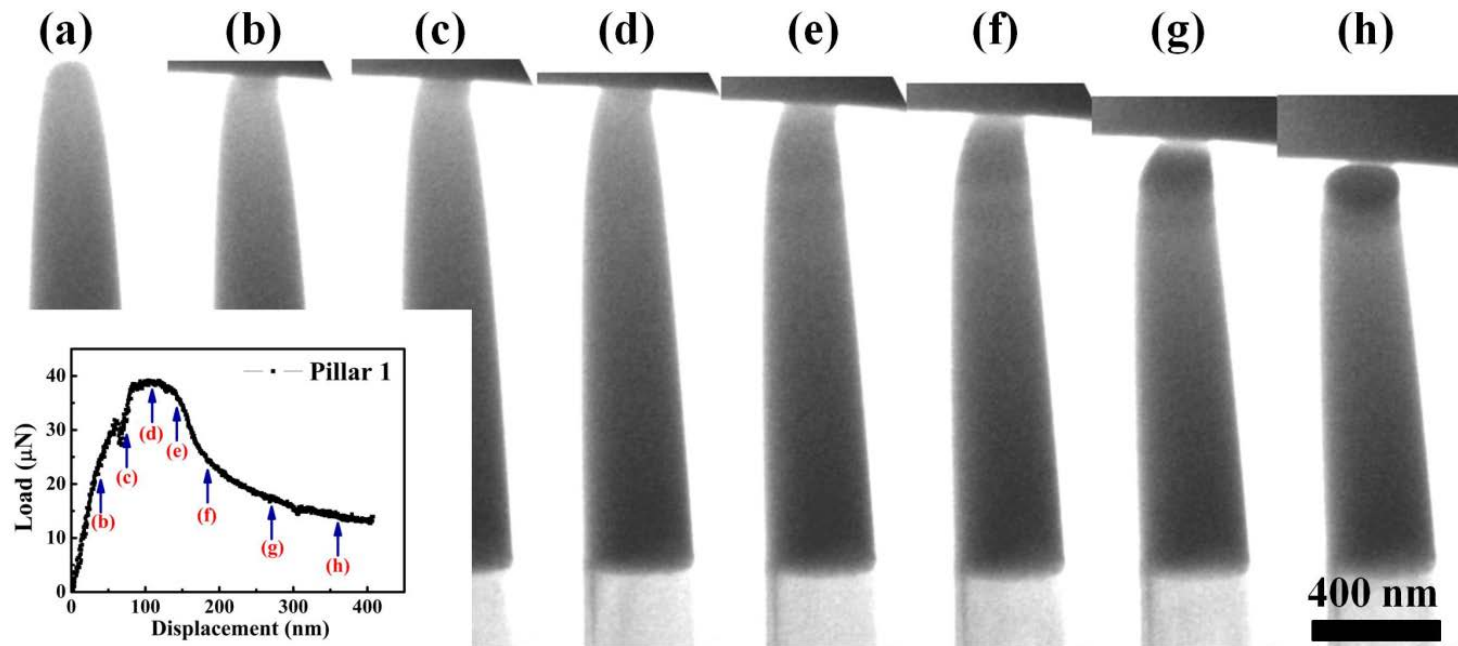
PI 95 TEM picoindenter holder

In situ TEM compression tests



Representative load-displacement curves of the in situ TEM nanocompression tests on the ZrCu thin film metallic glass nanopillars, 140 nm in diameter.

In situ TEM compression tests



Video snaps taken from the in-situ TEM compression showing the deformation of Zr-based pillar (Pillar 1). The different stages of the nanocompression process are depicted by individual frames [(a)-(h)] at different strains: **(a) undeformed, (b) ~2%, (c) ~4%, (d) ~6%, (e) ~8%, (f) ~10%, (g) ~15%, and (h) ~20%.**

Effect of sample size

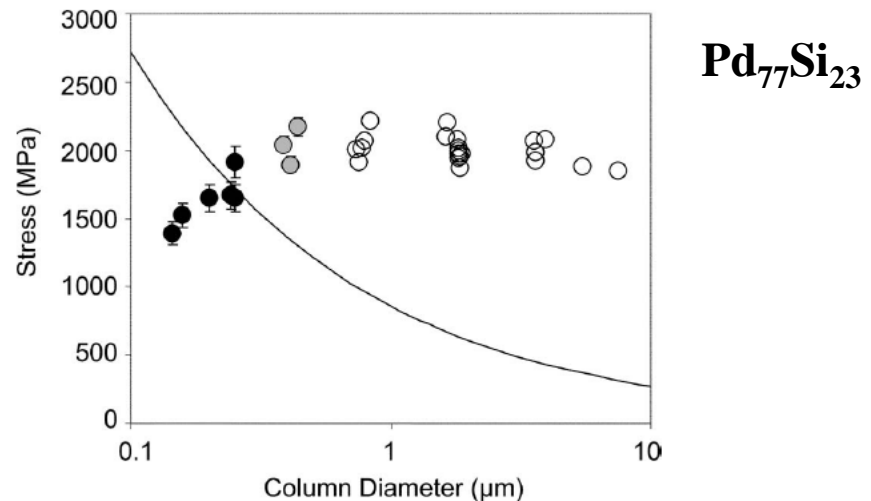
The elastic strain energy of the column is decreased by an amount $\pi\sigma\epsilon r^2 h/2$.

(where σ , ϵ , r , and h is stress, strain, pillar diameter, and shear band thickness)

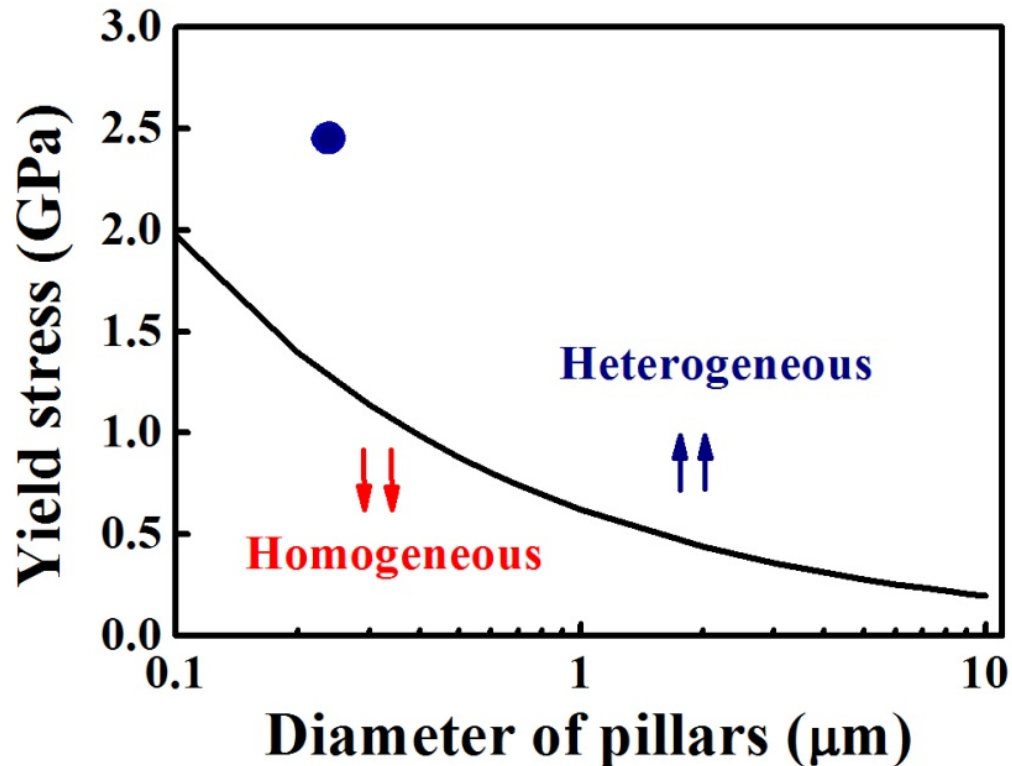
The shear band energy is increased by an amount $(2^{1/2}\pi r^2 \Gamma)^{1/2}$.
(where Γ is the energy per unit area of shear band.)

Estimation of the critical stress required for shear band formation

➔ $\sigma = (2^{3/2}\Gamma E/h)^{1/2}$

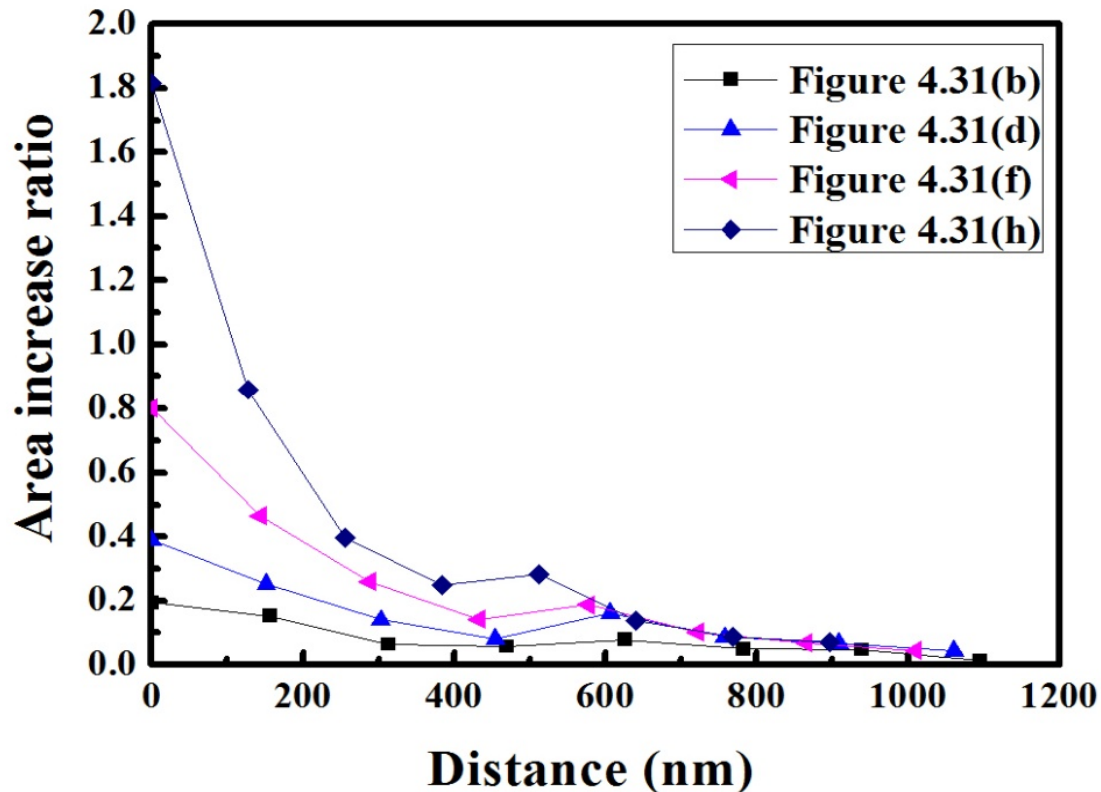


Effect of sample size



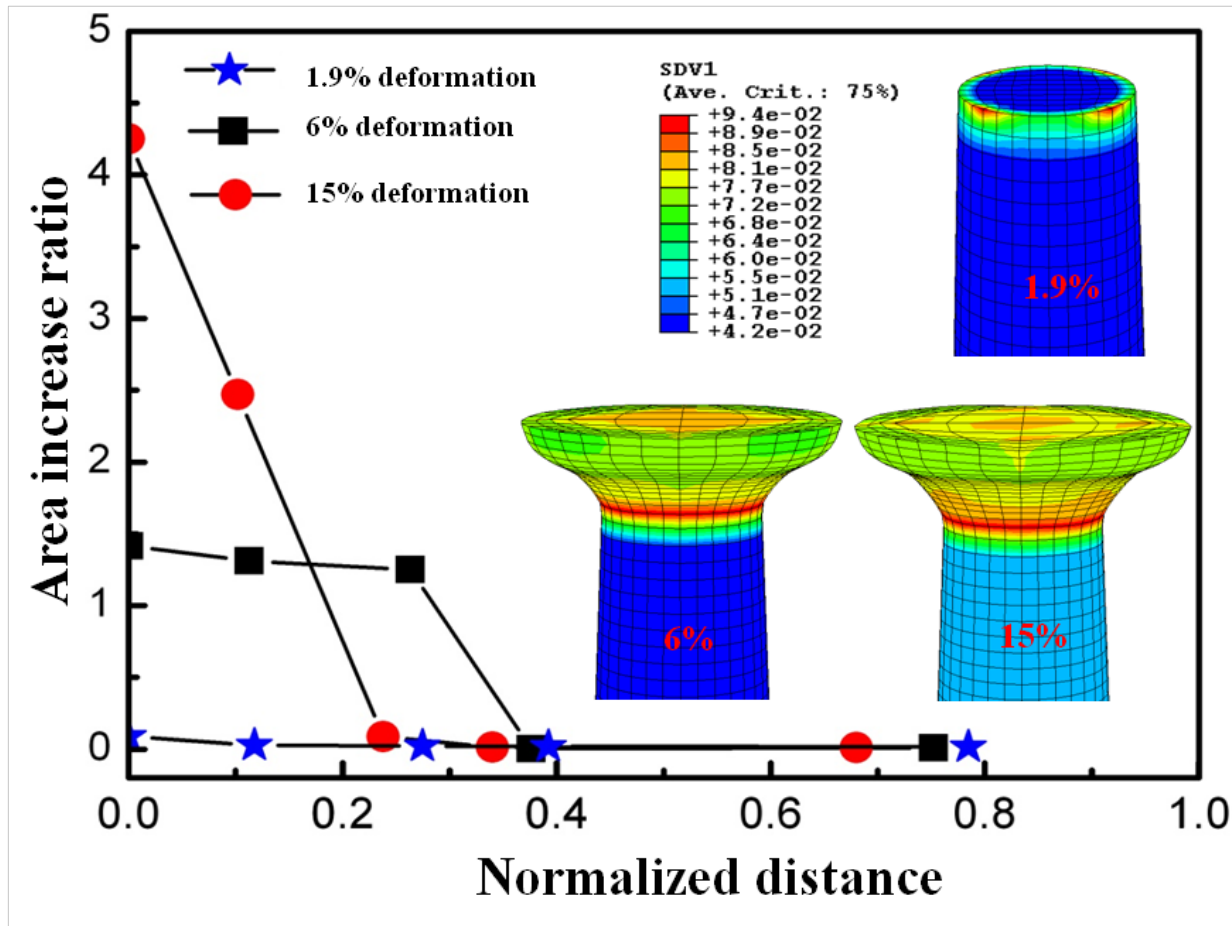
The calculated solid line showing the estimate of the minimum stress required to raise the strain energy high enough to allow for shear band formation.

In situ TEM compression tests



Change in cross-sectional area versus distance for Figures 4.31(b), (d), (f), and (h). Distance stands for distance the top of the pillar sample.

Finite element simulations



Area change ratio as a function of the distance from the specimen top (normalized by the base diameter) at three representative deformation stages with free volume contours in the insets.